Am J Cancer Res 2023;13(9):4222-4234
www.ajcr.us /ISSN:2156-6976/ajcr0149634

Original Article

ATXN3 deubiquitinates YAP1 to promote tumor growth

Shengnan Wang[1,2], Kun Liu[2], Xiaohua Han[3], Yang Cheng[1,2], Emily Zhao[4], Daniel J Brat[2], Zhaolin Sun[1], Deyu Fang[2]

[1]College of Basic Medical Sciences, Dalian Medical University, Dalian 116044, Liaoning, China; [2]Department of Pathology, Northwestern University Feinberg School of Medicine, Chicago, IL 60611, USA; [3]Department of Physiology, School of Basic Medicine, Qingdao University, Ningxia Road 308, Qingdao 266071, Shandong, China; [4]Weinberg College of Arts and Sciences, Northwestern University, Evanston, IL 60201, USA

Received February 12, 2023; Accepted April 11, 2023; Epub September 15, 2023; Published September 30, 2023

Abstract: The ubiquitin-specific peptidase Ataxin-3 (ATXN3) has emerged as a potential oncogene in a variety of human cancers. However, the molecular mechanisms underlying how ATXN3 achieves its tumorigenic functions remain largely undefined. Herein, we report that targeted deletion of the ATXN3 gene in cancer cells by the CRISPR-Cas9 system resulted in decreased protein expression of Yes-associated protein 1 (YAP1) without altering its mRNA transcription. Interestingly, genetic ATXN3 suppression selectively inhibited the expression levels of YAP1 target genes including the connective tissue growth factor (*Ctgf*) and cysteine-rich angiogenic inducer 61 (*Cyr61*), both of which have important functions in cell adhesion, migration, proliferation and angiogenesis. Consequently, ATXN3 suppression resulted in reduced cancer cell growth and migration, which can also be largely rescued by YAP1 reconstitution. At the molecular level, ATNX3 interacts with the WW domains of YAP1 to protect YAP1 from ubiquitination-mediated degradation. Immunohistology analysis revealed a strong positive correlation between ATXN3 and YAP1 protein expression in human breast and pancreatic cancers. Collectively, our study defines ATXN3 as a previously unknown YAP1 deubiquitinase in tumorigenesis and provides a rationale for ATXN3 targeting in antitumor chemotherapy.

Keywords: ATXN3, YAP1, deubiqutinase, cancer

Introduction

Ubiquitination is a process of post-translational protein modification by covalent conjugation of ubiquitin to the target proteins, which can be involved in regulating a broad spectrum of biological functions including cell proliferation, differentiation and death. This process is catalyzed by ubiquitin ligases, a family of proteins with near 1000 gene members in mammals, to specifically ligate ubiquitin onto the lysine residues of the target proteins. This ubiquitination either drives their degradation or controls their biological functions independent of protein destruction [1, 2]. On the other hand, the conjugated ubiquitin on the target protein can be reversibly removed by a family enzyme, the ubiquitin-specific peptidases or deubiquitinases, thus protecting the target proteins from degradation [3]. The dysregulated expression and/or activation of both ubiquitin ligases and deubiquitinases are involved in tumorigeneses [1, 3]. We and others, for example, have recently demonstrated that the ubiquitin-specific peptidase 22 (USP22) expression is elevated in many, if not all types of human cancers [4]. USP22 overexpression drives its functions in activating oncogenic Myc, inhibiting the tumor suppressor p53 and protecting cyclins from ubiquitination-mediated degradation [5-7]. In addition, USP22 functions as an immune suppresser both extrinsically and intrinsically in tumor cells to antagonize the antitumor immunity [8-10]. ATXN3 is highly conserved and ubiquitously expressed in mammals, but is a relatively understudied deubiquitinase. Surprisingly, while biochemistry analysis revealed that ATXN3 is involved in the degradation of misfolded chaperone substrates, transcriptional regulation, cytoskeleton regulation, and maintenance of protein homeostasis. While mice with systemic ATXN3 genetic deletion have normal viability or fertility and adult ATXN3 knockout mice display no overt abnormalities, the polyglutamine repeat expansion in the C-terminus of the human ATXN3 protein leads to

Spinocerebellar Ataxia Type 3, an age-related neurodegenerative disease [11]. Similarly, transgenic expression of a human ATXN3 gene modified with an expanded 84 CAG repeat motif resulted in the development of Machado-Joseph disease-like pathogenesis [12]. Importantly, accumulated evidence suggests that the deubiquitinase ATXN3 is a potential oncogene in a variety of human cancers such as breast and liver cancers, implying ATXN3 is a potential chemotherapeutic target in cancer treatment [13, 14]. Therefore, the fact that mice with systemic ATXN3 deletion are largely normal suggests ATXN3 is a safe target [15]. However, the underlying molecular mechanisms in how ATXN3 promotes tumor development, progression, and metastasis remain unclear.

The transcriptional co-activators yes-associated protein (YAP) and its paralog PDZ-binding motif (TAZ) are fundamentally important in the regulation of development, metabolism, organ growth, positional sensing and tissue regeneration [16]. Multiple upstream pathways, mediated by ligand-activated G protein-coupled receptors, tyrosine kinase receptors, integrins and mechanical cues positively control the YAP/TAZ transcriptional co-activator activity [16]. In contrast, YAP1 activation is negatively regulated by the Hippo signaling pathway, which was initially identified through genetic mosaic screens of *D. melanogaster* by its suppression of tissue overgrowth. The Hippo pathway plays an important role in limiting adult tissue growth and regulating cell proliferation, differentiation and migration of developing organs and other physiological processes. In addition, dysregulation of the Hippo pathway leads to abnormal cell growth and neoplasia [17]. When the Hippo pathway is switched on, activated downstream kinases, such as LATS and CK1 phosphorylate YAP and trigger YAP1 degradation by the RING-finger family ubiquitin ligases β-TrCP and FBXW7 as well as the suppressor of cytokine signaling (SOCS)5 and SOCS6 [18-21]. When the kinase casades are inhibited, YAP1 can be dephosphorylated. The unphosphorylated YAP1 then translocates into the nucleus and interact with the TEA domain family member TEAD for transcription of downstream target genes such as *CTGF* and *CYR61* [22, 23]. High YAP activity has been shown to positively affect tumor cell proliferation, survival, stemness, invasiveness and metastatic behavior, as well as therapy resistance in different cancers [24]. A recent study reported that the ubiquitin-specific peptidase 9X (USP9X) targets YAP1 for deubiquitination and stabilization, thereby promoting breast cancer cell survival and progression [25]. However, the mechanisms in which trigger and maintain cancerous YAP1 activation are still largely unknown.

Our current study identified that the deubiquitinase ATXN3 interacts with YAP1 in multiple cancer cell lines and functions as a YAP1 deubiquitinase. Interestingly, instead of globally reducing YAP1 transcriptional activity, targeted ATXN3 deletion in cancer cells selectively inhibited its target genes involved in cell adhesion, migration, proliferation and angiogenesis. Consequently, ATXN3 suppression resulted in reduced cancer cell growth and migration, which can also be largely rescued by YAP1 reconstitution. Our study discovered ATXN3 as a previously unappreciated YAP1 activator in promoting cancer cell growth.

Results

CRISPR/Cas9-mediated ATXN3 deletion inhibited YAP1 expression and cancer cell growth

It has been shown that ATXN3 promotes cancer growth and metastasis [13, 14]. To determine the potential role of ATXN3 in tumorigenesis, we used a CRISPR approach to knockout ATXN3 in mouse triple negative breast cancer 4T1 cells. Western blotting confirmed the deletion of ATXN3 (**Figure 1A**, **1B**). Interestingly, targeted ATXN3 deletion resulted in a dramatic reduction in YAP1 protein levels without altering its mRNA expression (**Figure 1A-C**), implying that ATXN3 promotes YAP1 expression at post-transcriptional level. Importantly, this reduction in YAP1 protein expression by ATXN3 targeted deletion did not result in a global change in YAP1 downstream target genes, because while both *Ctgf* and *Cyr61* are significantly decreased, the levels of *Ccnd1*, *Bcl2* and *Axl* were unaltered (**Figure 1D**, **1E**). Both *Ctgf* and *Cyr61* are important for many biological processes and oncogenesis, including cell adhesion, migration, proliferation and angiogenesis [26, 27]. Indeed, the proliferation of 4T1 cells was dramatically reduced by ATXN3 deletion (**Figure 1F**). The reduction in ATXN3-null cell proliferation is unlikely due to the increased cell death, because the levels of PI^+ and Annexin V-positive

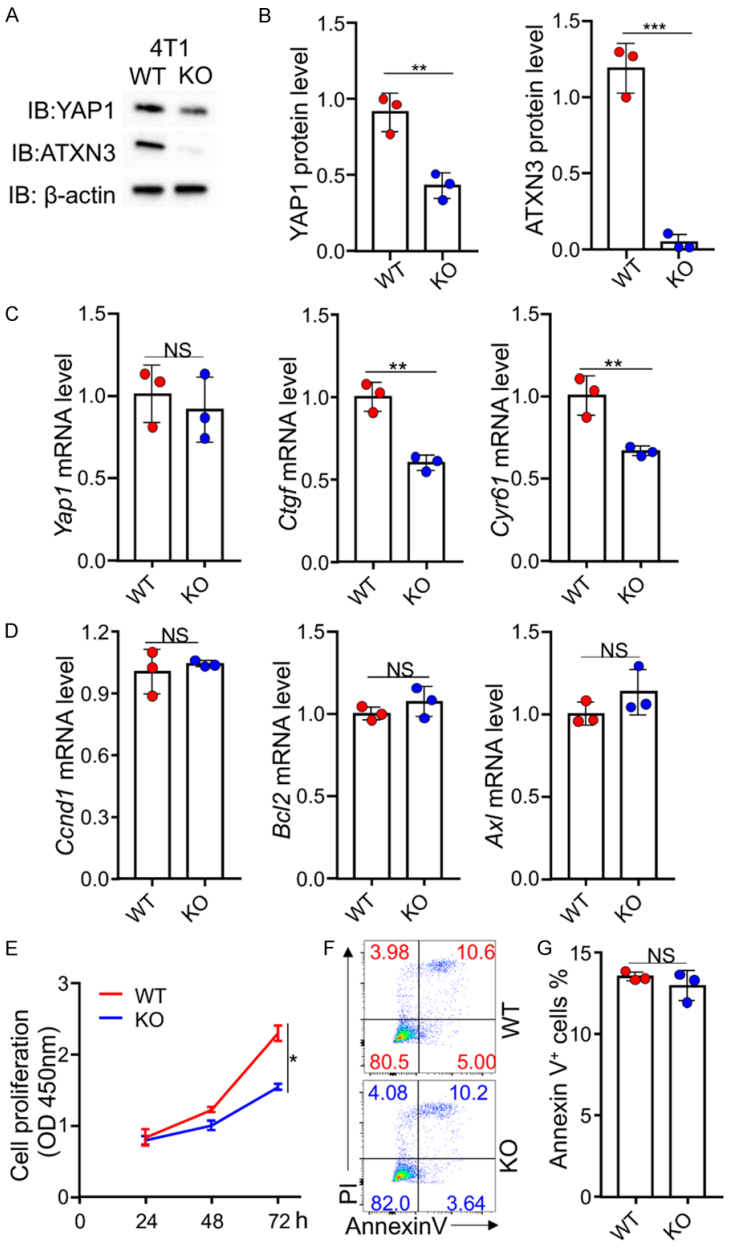

Figure 1. The effects of ATXN3 targeted deletion on breast cancer cell growth and death. (A, B) ATXN3 targeted deletion in triple negative breast 4T1 cells were generated. The protein levels of YAP1 (top panel), ATXN3 (middle panel) and loading control β-actin in WT and ATXN3 knockout 4T1 cells were determined by western blotting. Representative images (A) and quantitative analysis from 3 independent experiments (B) are shown. (C-E) The mRNA levels of *Yap1* (C) and its downstream target genes (D, E) in WT and ATXN3 knockout 4T1 cells were determined by real-time RT-PCR. (F, G) The effect of ATXN3 knockout on 4T1 proliferation was detected with WST-1 reagent (F) and their apoptosis was determined by PI and Annexin V staining (G). $^{*}P < 0.05$, $^{**}P < 0.01$, $^{***}P < 0.001$.

cells are incomparable between WT and ATXN3-null 4T1 cells (**Figure 1G**). Given the fact that elevated YAP1 activation promotes breast cancer growth [24], these results suggest that ATXN3 possibly promotes breast cancer growth through increasing YAP1 protein expression.

ATXN3 interacts with YAP1 in cancer cells

Because targeted deletion of the deubiquitinase ATXN3 reduced YAP1 protein expression at the post-transcriptional level, we hypothesized that ATXN3 was a possible YAP1 deubiquitinase. To test this, we first asked whether ATXN3 interacts with YAP1. Indeed, Myc-tagged ATXN3 was detected in the anti-Flag immunoprecipitants from HEK293 cells when both Myc-ATXN3 and Flag-YAP1 were transiently transfected, but not in cells transfected with Myc-ATXN3 alone (**Figure 2A**). More importantly, the interaction between endogenous YAP1 and ATXN3 was confirmed in multiple cancer cells including human lung adenocarcinoma A549, mouse breast cancer 4T1 and pancreatic cancer Panc-1 cells (**Figure 2B**), indicating ATXN3 possibly regulates YAP1 expression and transcriptional activation in a broad spectrum of cancer types. YAP1 has multiple domains including N-terminal TEAD transcription factor interaction domain (TID), two WW domains and a C-terminal transcriptional activation domain (TAD). Truncated mutation analysis indicated that neither the N-terminal TID nor its C-terminal TAD is involved in its interaction with ATXN3. Instead, the region with two WW domains mediates its interaction with ATXN3 (**Figure 2C**). Surprisingly, YAP1 interaction was detected with both the Josephin-domain containing N-terminal and the U19 peptidase domain carrying C-terminal truncated ATXN3 mutants (**Figure 2D**), implying that either both

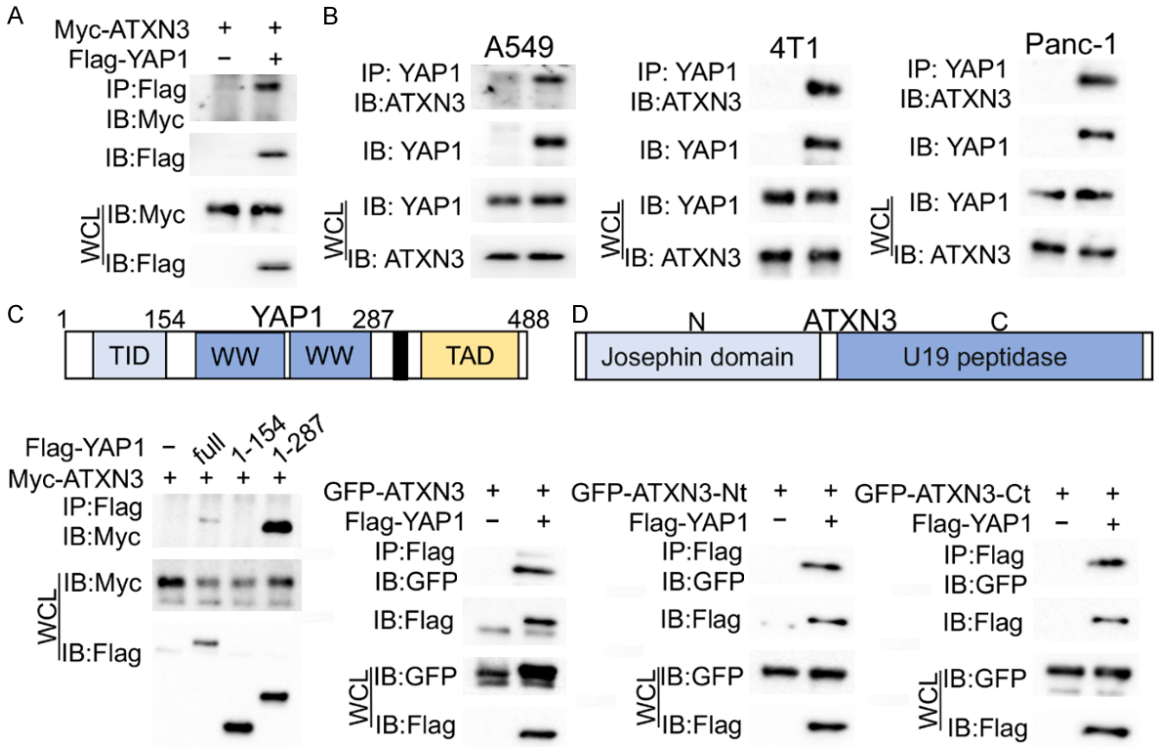

Figure 2. Analysis of ATXN3 interaction with YAP1. (A) Flag-YAP1 expression plasmid was transfected with or without Myc-ATXN3 expression plasmid. Their interaction was determined by immunoprecipitation with anti-Flag Abs and western blotting with anti-Myc (top panel). The membrane was reprobed with anti-Flag Abs (2nd panel). The expression levels of both Myc-ATXN3 and Flag-YAP1 in the whole cell lysates (WCL) were confirmed by western blotting (bottom panels). (B) The interaction between endogenous ATXN3 and YAP1 in each indicated cancer cell line was determined by immunoprecipitation with anti-YAP1 Abs and western bloting with anti-ATXN3 (top panel). The membrane was reprobed with anti-YAP1 Abs (2nd panel). The expression levels of both ATXN3 and YAP1 in the whole cell lysates were confirmed by western blotting (bottom panels). (C, D) The truncated mutation of ATXN3 and YAP1 was generated as indicated. Their interaction in transiently transfected HEK293 cells was determined as in (A).

domains or the junction region of ATXN3 mediate its interaction with YAP1.

ATXN3 deubiquitinates and stabilizes YAP1 in cancer cells

A deubiquitinase often inhibits the ubiquitination of its interacting proteins [28]. To test the possibility of ATXN3 regulation of YAP1 ubiquitination, HA-Ub plasmid was transiently transfected with Flag-YAP1 or further with Myc-ATXN3 into HEK293 cells. Following, YAP1 ubiquitination was determined as reported [29]. Higher molecular bands were detected in the anti-Flag immunoprecipitant when HA-Ub and Flag-YAP1 were co-expressed but not from HEK293 cells transfected with HA-Ub alone, indicating YAP1 is highly ubiquitinated presumably by its endogenous E3 ubiquitin ligase such as β-TrCP and FBXW7 [20, 21]. Of note, co-expression with ATXN3 largely diminished YAP1 ubiquitination (**Figure 3A**). As a consequence, ATXN3 co-expression significantly prolonged the half-life of YAP1 protein (**Figure 3B**, **3C**). Conversely, the half-life of YAP1 protein was dramatically shortened by ATXN3 targeted deletion in breast cancer 4T1 cells (**Figure 3D**, **3E**). Collectively, these data indicate that ATXN3 functions as a YAP1 deubiquitinase and enhances YAP1 activation in cancer cells.

When the inhibitory Hippo kinase signal is 'on', YAP1 is inactivated by phosphorylation and subsequently degradion by ubiquitination [30]. To examine whether ATXN3-mediated YAP1 deubiquitnation and stabolization is also phosphorylation dependent. We analyzed the level of p-YAP1 in WT and ATXN3 kockout cells. Indeed, similar to its total YAP1, the levels of phosphorylated YAP1 were dramatically reduced by ATXN3 targeted deletion (**Figure 3F**). Further analysis revealed a dramatic reduc-

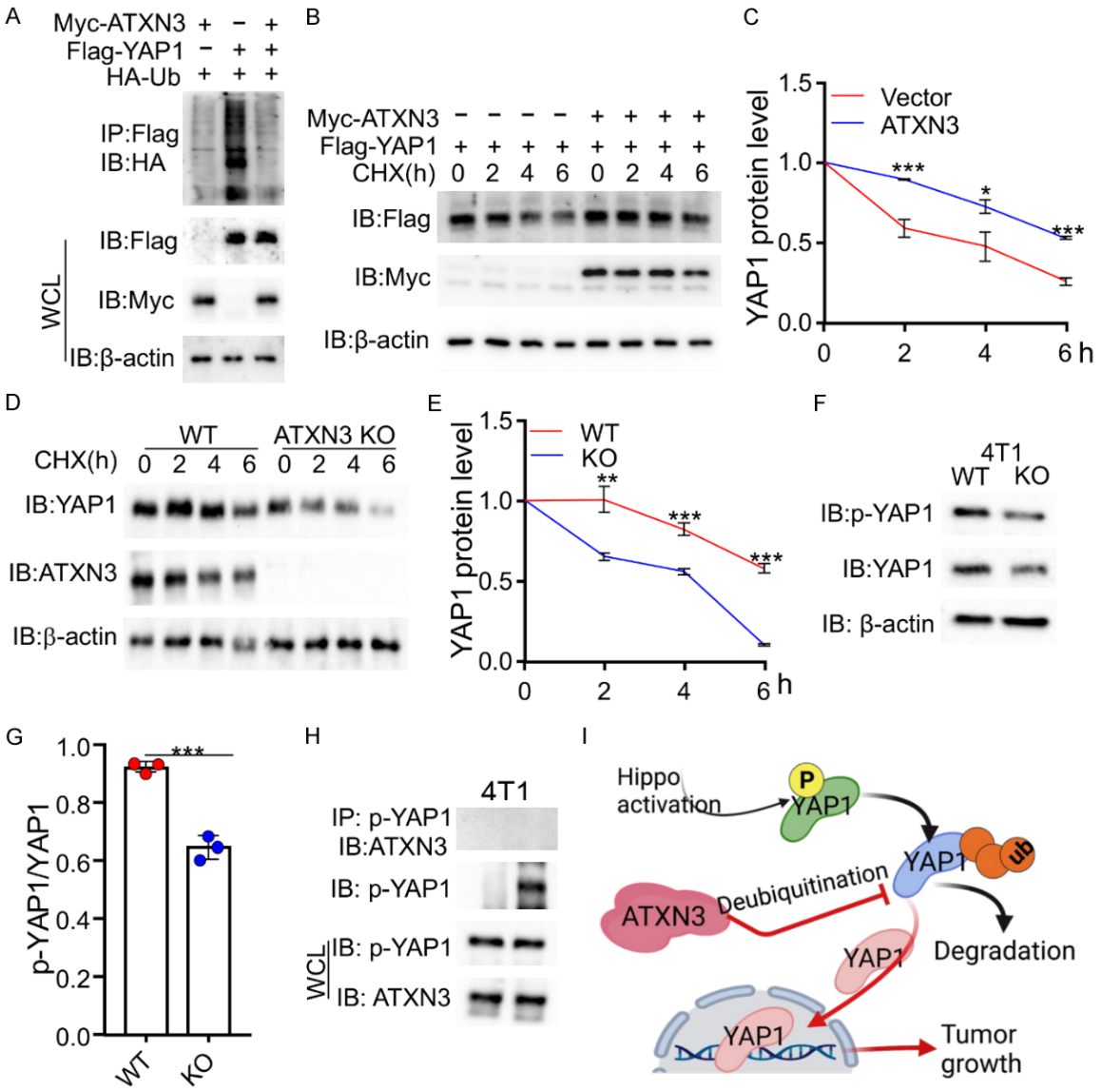

Figure 3. Analysis of ATXN3 effects on YAP1 ubiquitination and protein stability. (A) HA-Ub expression plasmid was co-transfected with or without Flag-YAP1 or further with Myc-ATXN3. YAP1 protein was pulled down by anti-Flag Abs and its ubiquitination was determined by western blotting with anti-HA Abs (top panel). The expression levels of both Myc-ATXN3 and Flag-YAP1 in the whole cell lysates (WCL) were confirmed by western blotting (bottom panels). (B, C) Flag-YAP1 was co-transfected with or without Myc-ATXN3 into HEK293 cells. Two days after transfection, cells were treated with cycloheximide (CHX) for each indicated time. The expression levels of YAP1 (top) and ATXN3 (bottom) were determined by western blotting. Representative images (B) and quantitative analysis from 3 independent experiments (C) are shown. (D, E) The effects of endogenous ATXN3 deletion on YAP1 protein stability in 4T1 cells were determined as in (B, C). $^{*}P < 0.05$, $^{**}P < 0.01$, $^{***}P < 0.001$. (F, G) The protein levels of p-YAP1, YAP1 and loading control β-actin in WT and ATXN3 knockout 4T1 cells were determined by western blotting, and quantitative analysis from 3 independent experiments are shown in (G). (H) The interaction of endogenous ATXN3 and p-YAP1 in 4T1 cells. (I) ATXN3 suppression facilitates the degradation of phosphorylated YAP1, but ATXN3 interaction is independent of YAP1 phosphorylation. $^{*}P < 0.05$, $^{**}P < 0.01$, $^{***}P < 0.001$.

tion in the ratio of phosphorylated YAP1 to total YAP1 (**Figure 3G**). However, analysis of the ATXN3-binding YAP1 did not detect any p-YAP1 (**Figure 3H**). These results indicated that ATXN3 suppression facilitates the degradation of phosphorylated YAP1, but ATXN3 interaction is independent of YAP1 phosphorylation (**Figure 3I**).

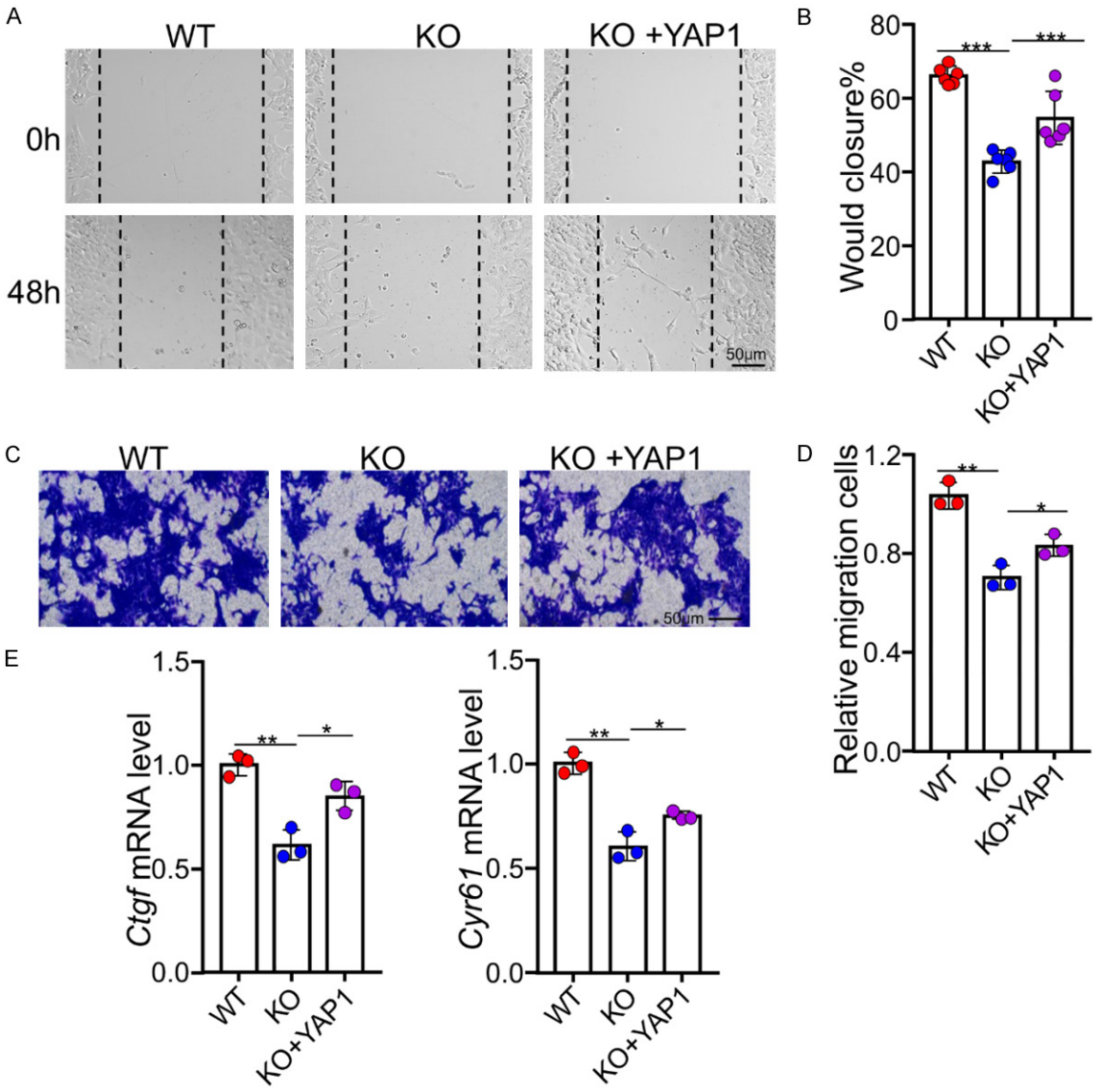

Figure 4. Analysis of ATXN3 effects on 4T1 breast cancer cell migration. A, B. Typical optical images of wound healing assessments in WT and ATXN3 KO 4T1 cells transfected with or without YAP1 plasmid. Percentage wound closure was determined by calculating the invaded area at 48 h to that at time 0 h. C, D. The migration ability of 4T1 cells was detected by transwell assay. The percentage of migration cells were quantified and normalized by control group. E. The mRNA levels of *Ctgf* and *Cyr61* genes in WT and ATXN3 knockout 4T1 cells after transfected with or without YAP1 were determined by real-time RT-PCR. $^{*}P < 0.05$, $^{**}P < 0.01$, $^{***}P < 0.001$.

ATXN3 promotes cancer cell migration in a YAP1-dependent manner

Our results indicate that ATXN3 functions as a deubiquitinase to selectively promote YAP1 target gene *Ctgf* and *Cyr61* expression, both of which are important for oncogenesis, with functions in cell adhesion, migration, proliferation and angiogenesis [26]. Indeed, ATXN3 deletion greatly decreased cell migration abilities compared with the control as inhibition of ATXN3 expression resulted in a slower gap filling rate in the wound-healing assay. Importantly, YAP1 overexpression largely rescued the migration abilities of ATXN3-null 4T1 cancer cells (**Figure 4A**, **4B**). Moreover, the number of migration cells was significantly decreased by ATXN3 deletion in the transwell migration assay, which was also largely rescued by YAP1 overexpression (**Figure 4C**, **4D**). These results indicate that ATXN3 promotes 4T1 cell migration and growth at least partially in a YAP1-dependent manner.

To support this conclusion, we further demonstrated that YAP1 expression in ATXN3-null cells rescued the expression levels of *Ctgf* and *Cyr61* target genes that are important for cancer cell growth and migration (**Figure 4E**). Unbiased analysis the TCGA database revealed a modest but statistically significant positive correlation between *ATXN3* and YAP1 targets, *CYR61* (r=0.3) and *CTGF* (r=0.244) mRNA levels in pancreatic cancer, but not in breast cancer (Figure S1).

ATXN3 and YAP1 expression is positively correlated in human breast cancer and pancreatic cancer

Our data collectively documented that ATXN3 is a YAP1 deubiquitinase that specifically promotes the expression of YAP1 target genes involved in cancer cell proliferation and migration. To further validate our findings in human cancers, we analyzed protein expression levels of ATXN3 and YAP1 in human breast and pancreatic cancers. As expected, the beast cancers with high ATXN3 expression often show a higher level of YAP1 protein expression, which show a modestly strong positive correlation with the r=0.3996 ($P < 0.001$) (**Figure 5A**, **5B**). A similar positive correlation between ATXN3 and YAP1 was confirmed in human pancreatic cancers (**Figure 5C**, **5D**). Therefore, our data support a link between ATXN3 and YAP1 in human cancer through, at least in part, protecting YAP1 from ubiquitination-induced protein degradation.

Discussion

The current study identifies ATXN3 as a YAP1 deubiquitinase to promote cancer cell growth and migration. This conclusion is documented by the following discoveries: First, targeted ATXN3 deletion inhibited YAP1 protein levels but not mRNA expression; second, ATXN3 selectively promoted the expression of YAP1 target genes involved in proliferation and migration; third, ATXN3 interacted with and protected YAP1 from ubiquitination-mediated degradation; fourth, impaired cancer cell migration by ATXN3 inhibition was largely rescued by YAP1 reconstitution. Last but not the least, ATXN3 positively correlated with YAP1 proteins in human breast and pancreatic cancers.

Several studies have shown that ATXN3 play an important role in the development and progression in multiple types of cancers including breast cancer [13, 31], anaplastic thyroid carcinoma [14], testicular cancer and non-small cell lung adenocarcinoma [32, 33] in a tumor cell-intrinsic manner. However, the exact role and underlying molecular mechanisms of ATXN3 in tumorigenesis still remain understudied. Few oncogenic substrates of ATXN3, including KLF4, EIF5A2 and PTEN have been identified in cancers. Our study here discovered that the oncogenic activation of YAP1 is potentiated by ATXN3 through removal of the polyubiquitination from YAP1, and consequently protecting it from ubiquitination-induced protein degradation. Importantly, the interaction between endogenous ATXN3 and YAP1 proteins was detected in multiple types of cancer cells, suggesting that ATXN3-mediated YAP1 stabilization and activation is involved in a variety cancer development.

One interesting question is, while ATXN3 targeted deletion dramatically reduced YAP1 protein expression, the transcription of YAP1 target genes was not globally decreased. This is possibly because ATXN3 may either regulate YAP1 activation in a target-specific manner, or YAP1 activates its target gene expression with different thresholds. Indeed, we have recently demonstrated that the deubiquitinase USP22 regulates gene transcription through suppressing histone 2B monoubiquitination in Tregs without altering H2A ubiquitination, another well-known target of USP22 [8]. YAP1 transcriptional activation relies on its nuclear translocation [34], and the accumulated YAP1 nuclear localization predicts poor clinical outcomes in many types of human cancers [35, 36]. It will be interesting to further investigate the subcellular localization of ATXN3 interaction with YAP1.

In addition to ATXN3, several deubiquitinating enzymes including the ubiquitin-specific peptidase 7 (USP7) [37], USP9X [38, 39], USP10 [40], USP47 [41], OTUB1 [42], and OTUB2 [43] stabilize YAP1 protein. As pointed out by the reviewer, fundamentally important questions behind this complexity, such as how these deubiquitinase crosstalk to control deubiquitination-mediated YAP1 stabilization, whether each of these deubiquitinases stabilize YAP1 to achieve a similar function? remain to be answered. Interestingly, similar to ATXN3 from our study, OTUB1 also interacts with the WW

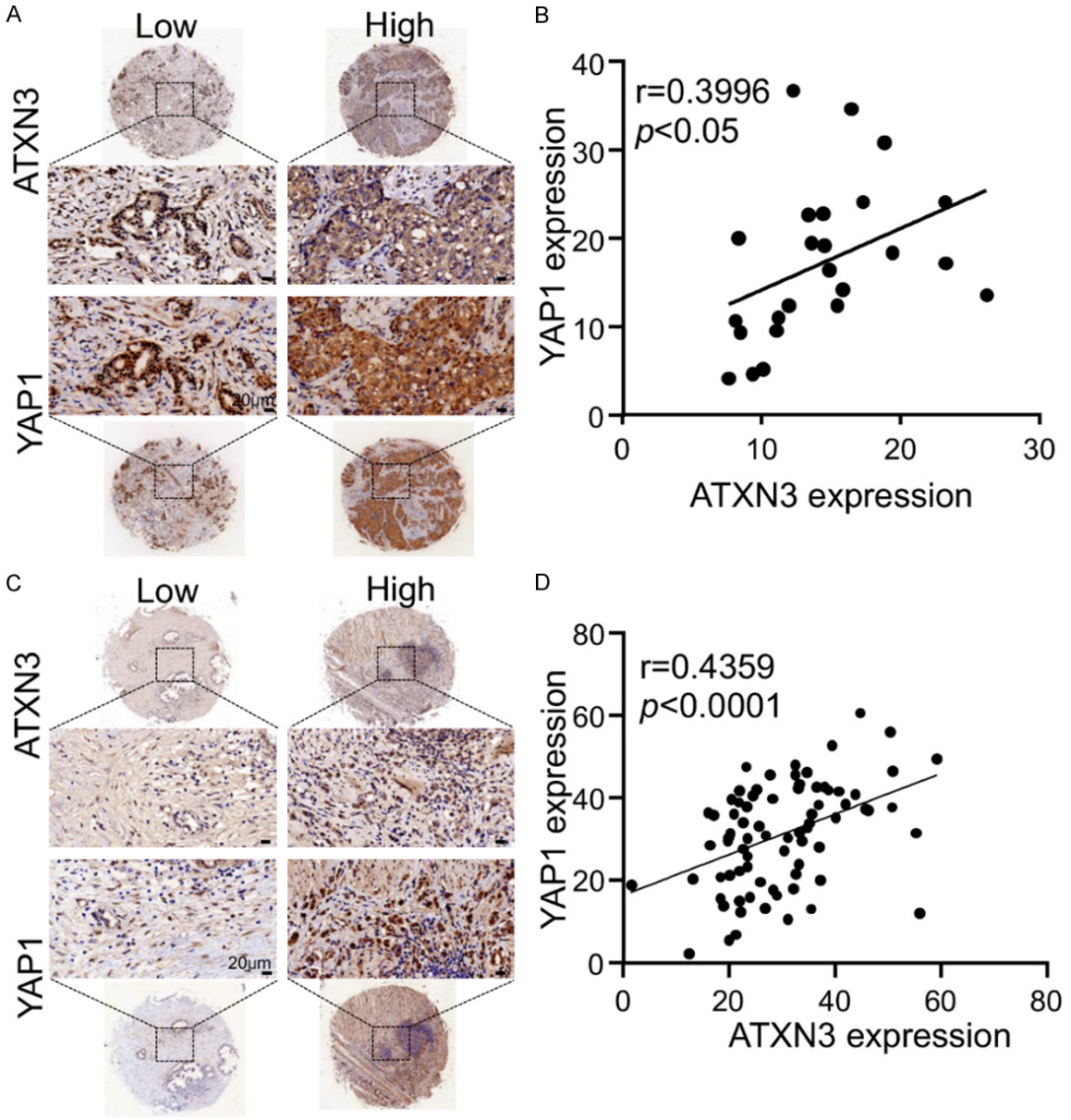

Figure 5. Analysis of ATXN3 correlation with YAP1 in human breast and pancreatic cancers. A, B. Representative images from IHC staining of ATXN3 and YAP1 in human breast cancer tissues are shown and their correlation were analyzed (n=24). C, D. Representative images from IHC staining of ATXN3 and YAP1 in human pancreatic cancer tissues are shown and their correlation were analyzed (n=39). $^{*}P < 0.05$, $^{**}P < 0.01$, $^{***}P < 0.001$.

domain-containing region of YAP1 [42]. In contrast, both USP7 and OTUB2 have been shown to recognize the N-terminus, but not the WW domain of YAP1 [37, 43]. While the regions in YAP1 that recognized by USP10 and USP47 have not been mapped [40, 41], it will be interesting to study whether, if yes, how these deubiquinases, such as ATXN3 and OTUB1, or USP7 and OTUB2, compete with the same region of YAP1 to regulate YAP1 transcriptional activation. In addition to YAP1, USP9X is an important regulator of the core kinases of Hippo pathway through deubiquinating LATS kinase, WW45, KIBRA, and Angiomotin, which consequently upregulating both YAP1 and its analog TAZ [44]. It is unclear whether ATXN3 regulates YAP1 and TAX in a similar fashion. Moreover, it is well accepted that YAP1 ubiquitination often occurs in the cytoplasm and is regulated by phosphorylation. Indeed, studies

have shown that USP9X [45], USP10 [46], USP47 [47] are predominantly localized in the cytoplasm. In contrast, USP7 shows exclusive nuclear colocalization [48]. Similar to ATXN3 [49], OTUB1 [50], and OTUB2 [51] can be distributed in both cytoplasm and nuclear of the cells. Therefore, future studies are needed to illustrate whether and how each of these deubiquitinases regulate YAP1 in a sub-cellular localization-specific manner. More importantly, YAP1 transcriptional activation is regulated by verity of important signaling including cell polarity, energy stresses, G-protein-coupled receptors, and stiffness of the extracellular matrix [52], it will be interesting and important to further dissect the extracellular signaling pathways differentially regulate each of the deubiquitinases in regulating YAP1 protein stability, subcellular localization and transcriptional activation at physiological and pathological contacts.

In summary, results from our study identifies a novel YAP1 deubiquitinase ATXN3 that drives cancer proliferation and migration. Thus, we provide a rationale for targeted therapeutic intervention of ATXN3 in the treatment of human cancers, in particular for those with elevated YAP1 activation.

Methods

Cell culture, transfection, generating stable cell line and cell treatment

HEK293, Panc-1 and A549 cells were cultured in Dulbecco's Modified Eagle Medium (DMEM) supplemented with 10% fetal bovine serum. 4T1 cells were maintained in RPMI 1640 with 10% FBS. Transfections were performed with Lipofectamine 3000 (Invitrogen, Cat#: L3000-150) according to the manufacturer's instructions. After 48 hours post-transfection, cells were harvested and subjected to various assays. For *Atxn3* gene knockout, cells were selected in the presence of puromycin (MCE, Cat#: HY-B1743Aa) for at least 2 days to generate stable cell lines. For cell degradation experiments, the transfected HEK293 cells or 4T1 cells were treated with cycloheximide (CHX) (Cell Signaling Technology, Cat#: 2112) for different times.

Plasmids and other reagents

Myc-ATXN3 (Cat#: RC218923) plasmid was purchased from Origene. LentiCRISPR v2 (Cat#: 25926), GFP-ATXN3 (Cat#: 89975), GFP-ATXN3 N-t (Cat#: 89980), GFP-ATXN3 C-t (Cat#: 89981) and pFlag-Yap1 (Cat#: 66853) were purchased from Addgene. Myc-ATXN3, pFlag-Yap1 (1-154 aa) and (1-287 aa) truncations were cloned by generating stop coding (Q5® Site-Directed Mutagenesis Kit, Cat#E0054S). SgRNA for mouse *Atxn3* was cloned into LentiCRISPR v2 vector.

Co-immunoprecipitation and western blotting

Cells were washed with ice-cold phosphate-buffered saline (PBS), lysed in RIPA lysis buffer with protease inhibitor and incubated on ice for 10 min, followed by centrifugation at 15000 g, 10 min. Supernatants were pre-cleaned with protein-G sepharose (GE Healthcare, Cat#: 17-0618-02) for 3 times, 20 min each time and subjected to immunoprecipitation with each indicated antibodies, incubated for 2 h on a shaker in cold room, and then added 50 μL of protein-G sepharose beads overnight. The beads were then washed for five times, boiled with 50 μL of 2 × loading buffer for 5 min and the proteins were separated on 8-10% SDS-PAGE gels and transferred to nitrocellulose membranes. The membranes were blocked in 5% fat-free dried milk in Tris-buffered saline with 0.5% Tween 20 (TBST) for 1 h. The membranes were then incubated in appropriate primary antibodies overnight at 4°C. Membranes were washed in TBST and then incubated in horseradish peroxidase (HRP)-conjugated secondary antibodies (EMD Millipore Corp, goat anti-rabbit IgG antibody, HRP conjugate, Cat#: 12-348; goat anti-mouse IgG antibody, HRP conjugate, Cat#: 12-349) for 1 h. Then membranes were washed in TBST, and the signals were visualized using enhanced chemiluminescence substrate (Thermo Scientific, Cat#: 34577) and quantified using the Bio-Rad Image software. Primary antibodies used are as follows: ATXN3 (Protein tech, Cat#: 67057-1-Ig), β-actin (Protein tech, Cat#: 66009-1-Ig), Flag-tag (Sigma, Cat#: F1804). Antibodies to GFP-tag (Cat#: 2956), Myc-tag (Cat#: 2278S), YAP1 (Cat#: 12395) and p-YAP1 (Cat#: 4991) were purchased from Cell Signaling Technology.

Real-time quantitative PCR with reverse transcription

Total RNA was extracted using the RNeasy Micro Kit (Qiagen, Cat#: 74106) and then

reversed-transcribed with the qScript cDNA synthesis kit (Quanta Bioscience, Cat#: 84003). Quantitative PCR was performed with the qScript cDNA Synthesis kit (Quanta Biosciences, Cat#: 95047-100). The mRNA level was calculated using the ΔCt method and normalized by *Actb*. Primers were purchased from Real Time Primers. All primers used for this study are listed in Table S1.

Cell proliferation assay

In vitro cell proliferation was measured by using the colorimetric WST-1 assay (cell proliferation reagent WST-1, Roche Diagnostics). Briefly, 2,000 4T1 cells were seeded in a 96-well plate with RPMI 1640 containing 10% fetal bovine serum. Every 24 h, 10 μL of WST-1 reagent was added to each well followed by incubation for 2 h. The absorbance at 450 nm was measured using a microplate reader.

Apoptosis assays

Cells were digested with Accutase solution (Corning, Cat#: 25-058-CI) and collected by centrifugation at 1500 × rpm for 5 min and washed cells twice with cold Annexin V bingding buffer buffer. Cells were stained in Annexin V bingding buffer (Biolegend, Cat#: 42201) with APC-AnnexinV (1:100, Biolegend, Cat#: 640-920) and PI (1:1000, Biolegend, Cat#: 79997) antibody. Subsequently, Cells were acquired on BD flow cytometry and data were analyzed using FlowJo software.

Wound-healing assay

4T1 cells were cultured in 6 wells and transfected with indicated plasmids. After 24 h post-transfection, the plate was scratched using a sterile 20 μl pipette tip and the pictures of scratches were taken respectively at 0 and 48 h. Image-J software was applied to analyze the scratch areas.

Transwell migration assay

Cell migration assay was performed in 24-well transwell plate with 12-mm polyethylene terephalate membrane filters (Corning) separating the lower and upper culture chambers. In brief, after 24 h post-transfection, 4T1 cells were plated in the upper chamber at 1×10^5 cells per well in serum-free RPMI 1640 medium. The bottom chamber contained RPMI 1640 medium with 20% FBS. Cells were allowed to migrate for 24 h in a humidified chamber at 37°C with 5% CO_2. After the incubation period, the filter was removed and non-migrant cells on the upper side of the filter were detached using a cotton swab. Filters were fixed with 4% formaldehyde for 20 min and cells located in the lower filter were stained with 0.2% crystal violet for 1 h and photographed.

Immunohistochemical (IHC) staining of tissue microarrays

Tumor tissue microarrays, purchased from Bioaitech Co.,Ltd (Cat#: D078Pa01, F048Br01), contain 39 pancreatic cancers cases and 24 breast cancers cases. Paraffin-embedded human tissue microarrays were deparaffinized, rehydrated, subjected to heat-induced antigen retrieval, blocked in goat serum blocking solution at room temperature for 30 min, and then incubated with primary antibodies overnight at 4°C. Primary antibodies used for IHC are antibodies against YAP1 (1:100, Cell Signaling Technology, Cat#: 12395), ATXN3 (1:500, Proteintech, Cat#: 13505-1-AP). The next day, the sections were washed and then incubated with biotin-conjugated secondary antibodies for 1 h at room temperature, and then the following used DAB chromogenic reaction. Then used hematoxylin stain solution for nucleus counterstaining and mounted. The images were captured using a Nikon microscope and analyzed by Aipathwell software. An H-score was calculated using the following formula: H-SCORE = $\sum$ (PI × I) = (percentage of cells of weak intensity × 1) + (percentage of cells of moderate intensity × 2) + (percentage of cells of strong intensity × 3). PI indicates the percentage of positive cells vs all cells, and I represents the staining intensity.

Statistical analyses

Statistical analysis was carried out using GraphPad Prism 7 software. Comparisons between groups were made by unpaired two-tailed Student's *t* test unless otherwise indicated, and $P < 0.05$ was considered significant. Pearson's correlation analysis was performed to determine the correlation between two variables.

Acknowledgements

We thank the Northwestern Lurie Cancer Center flow cytometry core for the service sup-

port. This work was supported by National Institutes of Health (NIH) grants R01DK126908, R01DK120330, R01CA257520 and CA232347 to D.F., the Shandong Province Natural Science Foundation ZR2019MH110 to X.H., as well as National Natural Science Foundation of China (No. 82073768) and Dalian High-level Talent Innovation Support Program (No. 2019RD03) to Z.S.

Disclosure of conflict of interest

None.

Address correspondence to: Zhaolin Sun, College of Basic Medical Sciences, Dalian Medical University, Dalian 116044, Liaoning, China. E-mail: zlsun56@yeah.net; Deyu Fang, Department of Pathology, Northwestern University Feinberg School of Medicine, Chicago, IL 60611, USA. E-mail: fangd@northwestern.edu

References

[1] Senft D, Qi J and Ronai ZA. Ubiquitin ligases in oncogenic transformation and cancer therapy. Nat Rev Cancer 2018; 18: 69-88.

[2] Bhattacharya A, Wei J, Song W, Gao B, Tian C, Wu SA, Wang J, Chen L, Fang D and Qi L. SEL1L-HRD1 ER-associated degradation suppresses hepatocyte hyperproliferation and liver cancer. iScience 2022; 25: 105183.

[3] Rawat R, Starczynowski DT and Ntziachristos P. Nuclear deubiquitination in the spotlight: the multifaceted nature of USP7 biology in disease. Curr Opin Cell Biol 2019; 58: 85-94.

[4] Melo-Cardenas J, Zhang Y, Zhang DD and Fang D. Ubiquitin-specific peptidase 22 functions and its involvement in disease. Oncotarget 2016; 7: 44848-44856.

[5] Lin Z, Yang H, Kong Q, Li J, Lee SM, Gao B, Dong H, Wei J, Song J, Zhang DD and Fang D. USP22 antagonizes p53 transcriptional activation by deubiquitinating Sirt1 to suppress cell apoptosis and is required for mouse embryonic development. Mol Cell 2012; 46: 484-494.

[6] Zhang XY, Varthi M, Sykes SM, Phillips C, Warzecha C, Zhu W, Wyce A, Thorne AW, Berger SL and McMahon SB. The putative cancer stem cell marker USP22 is a subunit of the human SAGA complex required for activated transcription and cell-cycle progression. Mol Cell 2008; 29: 102-111.

[7] Lin Z, Yang H, Tan C, Li J, Liu Z, Quan Q, Kong S, Ye J, Gao B and Fang D. USP10 antagonizes c-Myc transcriptional activation through SIRT6 stabilization to suppress tumor formation. Cell Rep 2013; 5: 1639-1649.

[8] Cortez JT, Montauti E, Shifrut E, Gatchalian J, Zhang Y, Shaked O, Xu Y, Roth TL, Simeonov DR, Zhang Y, Chen S, Li Z, Woo JM, Ho J, Vogel IA, Prator GY, Zhang B, Lee Y, Sun Z, Ifergan I, Van Gool F, Hargreaves DC, Bluestone JA, Marson A and Fang D. CRISPR screen in regulatory T cells reveals modulators of Foxp3. Nature 2020; 582: 416-420.

[9] Huang X, Zhang Q, Lou Y, Wang J, Zhao X, Wang L, Zhang X, Li S, Zhao Y, Chen Q, Liang T and Bai X. USP22 deubiquitinates CD274 to suppress anticancer immunity. Cancer Immunol Res 2019; 7: 1580-1590.

[10] Gregory S, Xu Y, Xie P, Fan J, Gao B, Mani N, Iyer R, Tang A, Wei J, Chaudhuri SM, Wang S, Liu H, Zhang B and Fang D. The ubiquitin-specific peptidase 22 is a deubiquitinase of CD73 in breast cancer cells. Am J Cancer Res 2022; 12: 5564-5575.

[11] Schols L, Vieira-Saecker AM, Schols S, Przuntek H, Epplen JT and Riess O. Trinucleotide expansion within the MJD1 gene presents clinically as spinocerebellar ataxia and occurs most frequently in German SCA patients. Hum Mol Genet 1995; 4: 1001-1005.

[12] Cemal CK, Carroll CJ, Lawrence L, Lowrie MB, Ruddle P, Al-Mahdawi S, King RH, Pook MA, Huxley C and Chamberlain S. YAC transgenic mice carrying pathological alleles of the MJD1 locus exhibit a mild and slowly progressive cerebellar deficit. Hum Mol Genet 2002; 11: 1075-1094.

[13] Zhu R, Gires O, Zhu L, Liu J, Li J, Yang H, Ju G, Huang J, Ge W, Chen Y, Lu Z and Wang H. TSPAN8 promotes cancer cell stemness via activation of sonic Hedgehog signaling. Nat Commun 2019; 10: 2863.

[14] Zhuang S, Xie J, Zhen J, Guo L, Hong Z, Li F and Xu D. The deubiquitinating enzyme ATXN3 promotes the progression of anaplastic thyroid carcinoma by stabilizing EIF5A2. Mol Cell Endocrinol 2021; 537: 111440.

[15] Schmitt I, Linden M, Khazneh H, Evert BO, Breuer P, Klockgether T and Wuellner U. Inactivation of the mouse Atxn3 (ataxin-3) gene increases protein ubiquitination. Biochem Biophys Res Commun 2007; 362: 734-739.

[16] Moroishi T, Hansen CG and Guan KL. The emerging roles of YAP and TAZ in cancer. Nat Rev Cancer 2015; 15: 73-79.

[17] Meng Z, Moroishi T and Guan KL. Mechanisms of Hippo pathway regulation. Genes Dev 2016; 30: 1-17.

[18] Nishioka N, Inoue K, Adachi K, Kiyonari H, Ota M, Ralston A, Yabuta N, Hirahara S, Stephenson RO, Ogonuki N, Makita R, Kurihara H, Morin-Kensicki EM, Nojima H, Rossant J, Nakao K, Niwa H and Sasaki H. The Hippo signaling pathway components Lats and Yap pattern

Tead4 activity to distinguish mouse trophectoderm from inner cell mass. Dev Cell 2009; 16: 398-410.
[19] Moya IM and Halder G. Hippo-YAP/TAZ signalling in organ regeneration and regenerative medicine. Nat Rev Mol Cell Biol 2019; 20: 211-226.
[20] Zhao B, Li L, Tumaneng K, Wang CY and Guan KL. A coordinated phosphorylation by Lats and CK1 regulates YAP stability through SCF (beta-TRCP). Genes Dev 2010; 24: 72-85.
[21] Tu K, Yang W, Li C, Zheng X, Lu Z, Guo C, Yao Y and Liu Q. Fbxw7 is an independent prognostic marker and induces apoptosis and growth arrest by regulating YAP abundance in hepatocellular carcinoma. Mol Cancer 2014; 13: 110.
[22] Johnson R and Halder G. The two faces of Hippo: targeting the Hippo pathway for regenerative medicine and cancer treatment. Nat Rev Drug Discov 2014; 13: 63-79.
[23] Zhao B, Ye X, Yu J, Li L, Li W, Li S, Yu J, Lin JD, Wang CY, Chinnaiyan AM, Lai ZC and Guan KL. TEAD mediates YAP-dependent gene induction and growth control. Genes Dev 2008; 22: 1962-1971.
[24] Szulzewsky F, Holland EC and Vasioukhin V. YAP1 and its fusion proteins in cancer initiation, progression and therapeutic resistance. Dev Biol 2021; 475: 205-221.
[25] Guo L, Chen Y, Luo J, Zheng J and Shao G. YAP1 overexpression is associated with poor prognosis of breast cancer patients and induces breast cancer cell growth by inhibiting PTEN. FEBS Open Bio 2019; 9: 437-445.
[26] Barreto SC, Ray A and Ag Edgar P. Biological characteristics of CCN proteins in tumor development. J BUON 2016; 21: 1359-1367.
[27] Rokkam P, Gugalavath S, Gift Kumar DK, Vempati RK and Malla RR. Prognostic role of Hedgehog-GLI1 signaling pathway in aggressive and metastatic breast cancers. Curr Drug Metab 2020; 21: 33-43.
[28] Zhang Y, Wang Y, Gao B, Sun Y, Cao L, Genardi SM, Wang CR, Li H, Sun Z, Yang Y and Fang D. USP22 controls iNKT immunity through MED1 suppression of histone H2A monoubiquitination. J Exp Med 2020; 217: e20182218.
[29] Yang Y, Kong S, Zhang Y, Melo-Cardenas J, Gao B, Zhang Y, Zhang DD, Zhang B, Song J, Thorp E, Zhang K, Zhang J and Fang D. The endoplasmic reticulum-resident E3 ubiquitin ligase Hrd1 controls a critical checkpoint in B cell development in mice. J Biol Chem 2018; 293: 12934-12944.
[30] Shen J, Huang Q, Jia W, Feng S, Liu L, Li X, Tao D and Xie D. YAP1 induces invadopodia formation by transcriptionally activating TIAM1 through enhancer in breast cancer. Oncogene 2022; 41: 3830-3845.
[31] Zou H, Chen H, Zhou Z, Wan Y and Liu Z. ATXN3 promotes breast cancer metastasis by deubiquitinating KLF4. Cancer Lett 2019; 467: 19-28.
[32] Sacco JJ, Yau TY, Darling S, Patel V, Liu H, Urbé S, Clague MJ and Coulson JM. The deubiquitylase Ataxin-3 restricts PTEN transcription in lung cancer cells. Oncogene 2014; 33: 4265-4272.
[33] Shi Z, Chen J, Zhang X, Chu J, Han Z, Xu D, Gan S, Pan X, Ye J and Cui X. Ataxin-3 promotes testicular cancer cell proliferation by inhibiting anti-oncogene PTEN. Biochem Biophys Res Commun 2018; 503: 391-396.
[34] Kuge S, Jones N and Nomoto A. Regulation of yAP-1 nuclear localization in response to oxidative stress. EMBO J 1997; 16: 1710-1720.
[35] Debaugnies M, Sanchez-Danes A, Rorive S, Raphael M, Liagre M, Parent MA, Brisebarre A, Salmon I and Blanpain C. YAP and TAZ are essential for basal and squamous cell carcinoma initiation. EMBO Rep 2018; 19: e45809.
[36] Howard A, Bojko J, Flynn B, Bowen S, Jungwirth U and Walko G. Targeting the Hippo/YAP/TAZ signalling pathway: novel opportunities for therapeutic interventions into skin cancers. Exp Dermatol 2022; 31: 1477-1499.
[37] Sun X, Ding Y, Zhan M, Li Y, Gao D, Wang G, Gao Y, Li Y, Wu S, Lu L, Liu Q and Zhou Z. Usp7 regulates Hippo pathway through deubiquitinating the transcriptional coactivator Yorkie. Nat Commun 2019; 10: 411.
[38] Li L, Liu T, Li Y, Wu C, Luo K, Yin Y, Chen Y, Nowsheen S, Wu J, Lou Z and Yuan J. The deubiquitinase USP9X promotes tumor cell survival and confers chemoresistance through YAP1 stabilization. Oncogene 2018; 37: 2422-2431.
[39] Toloczko A, Guo F, Yuen HF, Wen Q, Wood SA, Ong YS, Chan PY, Shaik AA, Gunaratne J, Dunne MJ, Hong W and Chan SW. Deubiquitinating enzyme USP9X suppresses tumor growth via LATS kinase and core components of the hippo pathway. Cancer Res 2017; 77: 4921-4933.
[40] Zhu H, Yan F, Yuan T, Qian M, Zhou T, Dai X, Cao J, Ying M, Dong X, He Q and Yang B. USP10 promotes proliferation of hepatocellular carcinoma by deubiquitinating and stabilizing YAP/TAZ. Cancer Res 2020; 80: 2204-2216.
[41] Pan B, Yang Y, Li J, Wang Y, Fang C, Yu FX and Xu Y. USP47-mediated deubiquitination and stabilization of YAP contributes to the progression of colorectal cancer. Protein Cell 2020; 11: 138-143.
[42] Yan C, Yang H, Su P, Li X, Li Z, Wang D, Zang Y, Wang T, Liu Z, Bao Z, Dong S, Zhuang T, Zhu J and Ding Y. OTUB1 suppresses Hippo signaling via modulating YAP protein in gastric cancer. Oncogene 2022; 41: 5186-5198.

[43] Zhang Z, Du J, Wang S, Shao L, Jin K, Li F, Wei B, Ding W, Fu P, van Dam H, Wang A, Jin J, Ding C, Yang B, Zheng M, Feng XH, Guan KL and Zhang L. OTUB2 promotes cancer metastasis via hippo-independent activation of YAP and TAZ. Mol Cell 2019; 73: 7-21, e7.

[44] Thanh Nguyen H, Andrejeva D, Gupta R, Choudhary C, Hong X, Eichhorn PJ, Loya AC and Cohen SM. Deubiquitylating enzyme USP9x regulates hippo pathway activity by controlling angiomotin protein turnover. Cell Discov 2016; 2: 16001.

[45] Wang Q, Tang Y, Xu Y, Xu S, Jiang Y, Dong Q, Zhou Y and Ge W. The X-linked deubiquitinase USP9X is an integral component of centrosome. J Biol Chem 2017; 292: 12874-12884.

[46] Yuan J, Luo K, Zhang L, Cheville JC and Lou Z. USP10 regulates p53 localization and stability by deubiquitinating p53. Cell 2010; 140: 384-396.

[47] Cho J, Park J, Shin SC, Jang M, Kim JH, Kim EE and Song EJ. USP47 promotes tumorigenesis by negative regulation of p53 through deubiquitinating ribosomal protein S2. Cancers (Basel) 2020; 12: 1137.

[48] Luo M, Zhou J, Leu NA, Abreu CM, Wang J, Anguera MC, de Rooij DG, Jasin M and Wang PJ. Polycomb protein SCML2 associates with USP7 and counteracts histone H2A ubiquitination in the XY chromatin during male meiosis. PLoS Genet 2015; 11: e1004954.

[49] Tait D, Riccio M, Sittler A, Scherzinger E, Santi S, Ognibene A, Maraldi NM, Lehrach H and Wanker EE. Ataxin-3 is transported into the nucleus and associates with the nuclear matrix. Hum Mol Genet 1998; 7: 991-997.

[50] Shan TL, Tang ZL, Guo DZ, Yang SL, Mu YL, Ma YH, Guan WJ and Li K. Partial molecular cloning, characterization, and analysis of the subcellular localization and expression patterns of the porcine OTUB1 gene. Mol Biol Rep 2009; 36: 1573-1577.

[51] Kato K, Nakajima K, Ui A, Muto-Terao Y, Ogiwara H and Nakada S. Fine-tuning of DNA damage-dependent ubiquitination by OTUB2 supports the DNA repair pathway choice. Mol Cell 2014; 53: 617-630.

[52] Pobbati AV, Kumar R, Rubin BP and Hong W. Therapeutic targeting of TEAD transcription factors in cancer. Trends Biochem Sci 2023; 48: 450-462.

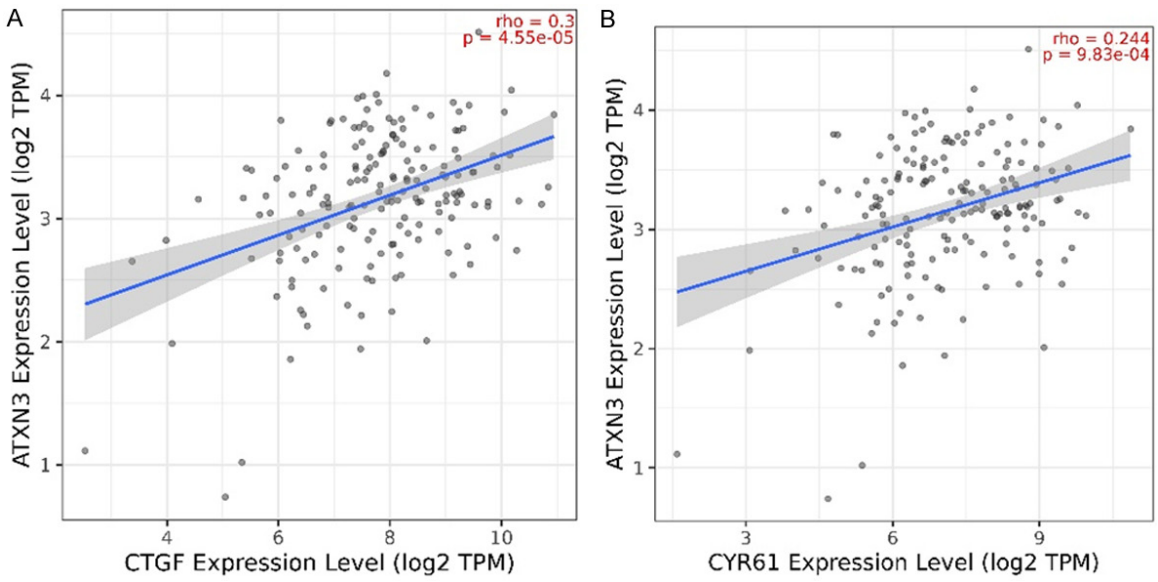

Figure S1. A, B. Correlation between *ATXN3*, *CTGF* and *CYR61* expression in PAAD from TCGA database.

Table S1. Primers used for this study

Species	Primer name	Sequence (5' to 3')	Purpose
mouse	*Yap1*	CCCTCGTTTTGCCATGAACC (Forward)	RT-qPCR
		ATTCCGTATTGCCTGCCGAA (Reverse)	
mouse	*Ctgf*	GGACACCTAAAATCGCCAAGC (Forward)	
		ACTTAGCCCTGTATGTCTTCACA (Reverse)	
mouse	*Cyr61*	TAAGGTCTGCGCTAAACAACTC (Forward)	
		CAGATCCCTTTCAGAGCGGT (Reverse)	
mouse	*Atxn3*	AAGTCGCCAGGAAATCGACA (Forward)	
		GCTGCTGCTGTTGCTTTTCAA (Reverse)	
mouse	*Ccnd1*	AAAATGCCAGAGGCGGATGA (Forward)	
		CAGGGCCTTGACCGGG (Reverse)	
mouse	*Actb*	TATAAAACCCGGCGGCGCA (Forward)	
		TCATCCATGGCGAACTGGTG (Reverse)	
mouse	*Bcl2*	CACCCCTGGTGGACAACATC (Forward)	
		TATAGTTCCACAAAGGCATCCCAG (Reverse)	
mouse	*Axl*	AGGAGCCCAGGGGTGG (Forward)	
		CCTCGGTCTGTGTGTCCTTA (Reverse)	
mouse	*Atxn3*	CACCGCAATTGAGGATAGCTCCAC (Forward)	CRISPR
		CACCGGCTCTAGCCATAAGTCGCC (Reverse)	